Electronic Supplementary Material (ESI) for Nanoscale.

Supplementary Information

Nacre-inspired Integrated Strong and Tough Reduced Graphene Oxide-Poly(acrylic acid) Nanocomposites

Sijie Wan[1†], Han Hu[1†], Jingsong Peng[1†], Yuchen Li[2†], Yuzun Fan[1], Lei Jiang[1] and Qunfeng Cheng[1,3*]

[1]Key Laboratory of Bio-inspired Smart Interfacial Science and Technology of Ministry of Education, School of Chemistry Environment, BeiHang University, Beijing, 100191, P. R. China

[2]Beijing Engineering Research Center of Printed Electronics, Beijing Institute of Graphic Communication, Beijing 102600, P. R. China

[3]State Key Laboratory for Modification of Chemical Fibers and Polymer Materials, Donghua University, Shanghai 201620, P. R. China

* To whom correspondence should be addressed. E-mail: cheng@buaa.edu.cn

† These authors contributed equally to this work.

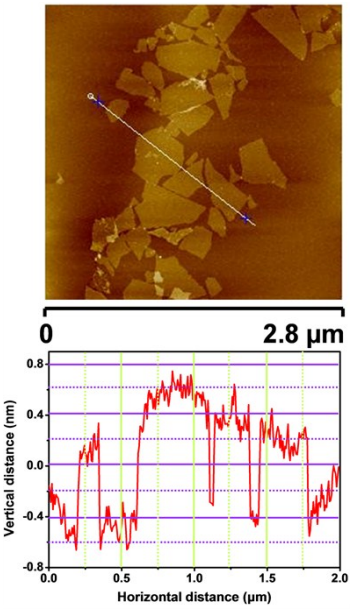

Figure S1. AFM image of as-prepared GO sheets and corresponding height profile, showing the thickness and lateral size of GO sheets to be 0.75 nm and 0.2~0.8 μm, respectively.

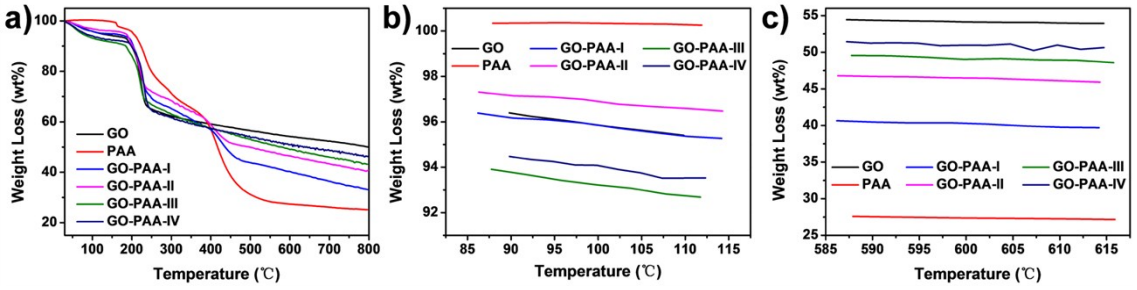

Figure S2. (a) TGA curves of pure GO and PAA films and GO-PAA nanocomposites under nitrogen atmosphere with a temperature rising rate of 10 K•min^{-1}. The high resolution of TGA curves with temperature at ~100°C (b) and ~600°C (c).

The weight loss was mainly resulted from the water evaporation before 100°C, both PAA and GO have all degradation peaks before 600 °C as clearly shown by the TGA curves in Figure S2a. Thus, the desired temperature were

decided to range from 100 °C to 600 °C to calculate the GO weight fraction in GO-PAA nanocomposites. The high resolution of TGA curves with temperature at ~100°C and ~600°C have also been plotted as shown in Figure S2b and S2c. The GO weight fraction (*w*) in GO-PAA nanocomposites could be determined by following equation:

$$\omega = \frac{M - M_{PAA}}{M_{GO} - M_{PAA}} \times 100\%$$

In this equation, *w* represents the GO weight fraction; *M*, M_{PAA} and M_{GO} are the weight loss of GO-PAA nanocomposites, pure PAA film and GO film between 100°C and 600°C, respectively. The detail data for M_{PAA}, M_{GO} and *M* for each GO-PAA nanocomposite were listed in Table S1.

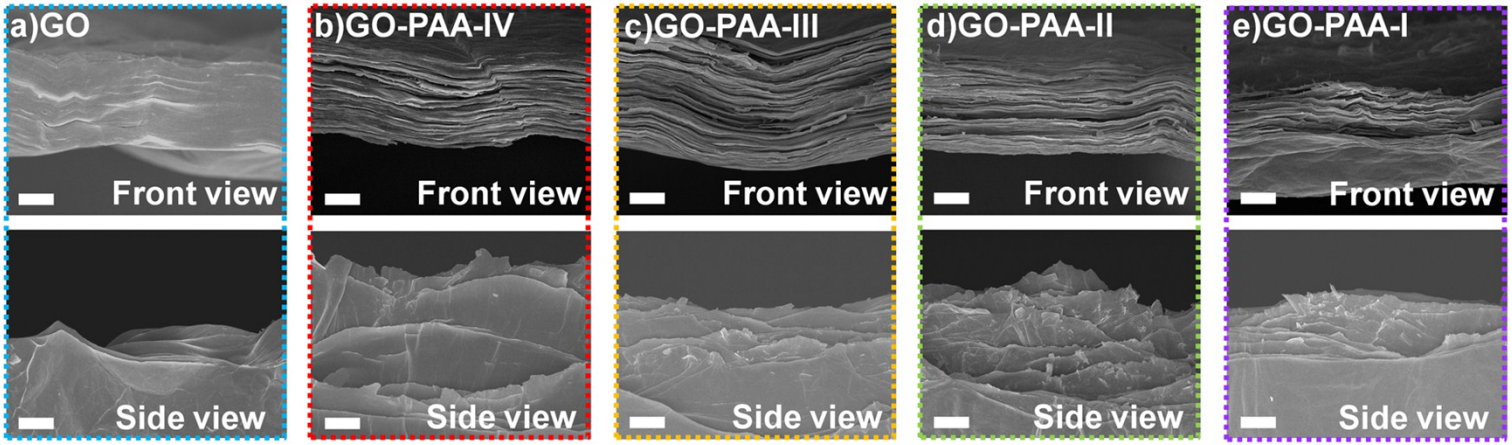

Figure S3. Fracture morphology of GO and GO-PAA nanocomposites with different GO contents: a) GO film, b) GO-PAA-IV, c) GO-PAA-III, d) GO-PAA-II and e) GO-PAA-I. The scale bar is 2 μm.

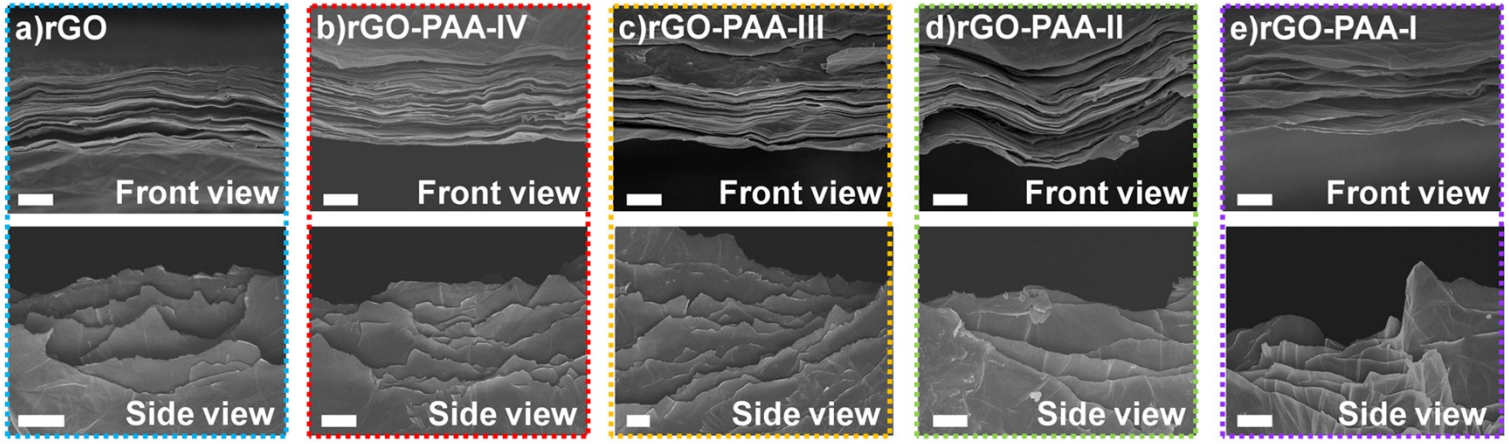

Figure S4. Fracture morphology of rGO and rGO-PAA nanocomposites with different GO contents: a) rGO film, b) rGO-PAA-IV, c) rGO-PAA-III, d) rGO-PAA-II and e) rGO-PAA-I. The scale bar is 2 μm.

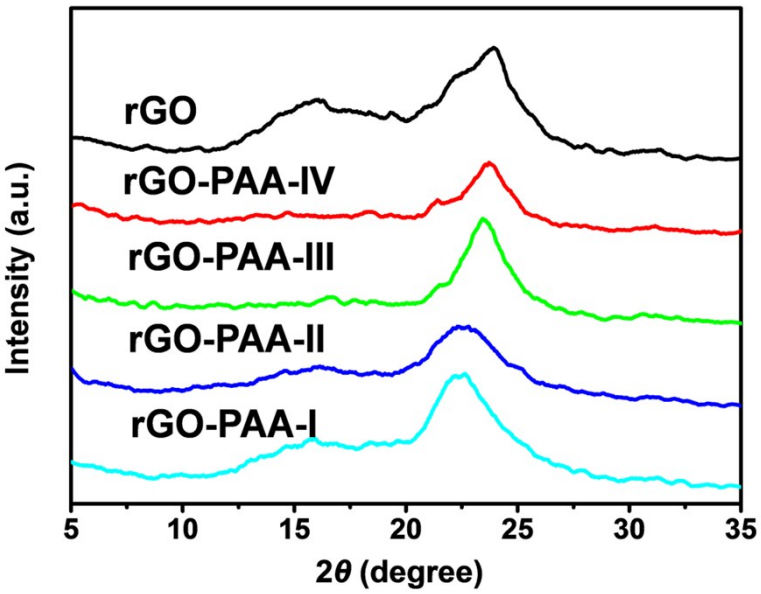

Figure S5. X-ray diffraction (XRD) curves of pure rGO film and rGO-PAA nanocomposites.

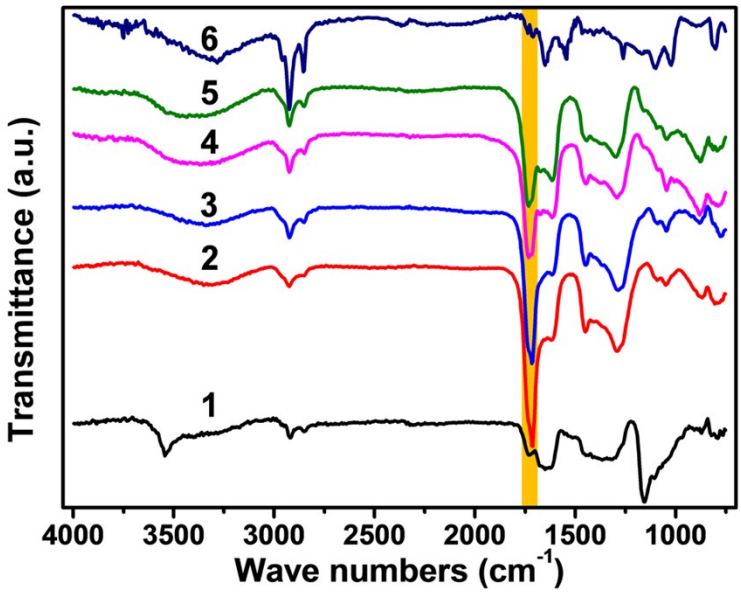

Figure S6. FTIR spectra of pure rGO (1) film, rGO-PAA I-IV (2-5) nanocomposites and pure PAA (6) film.

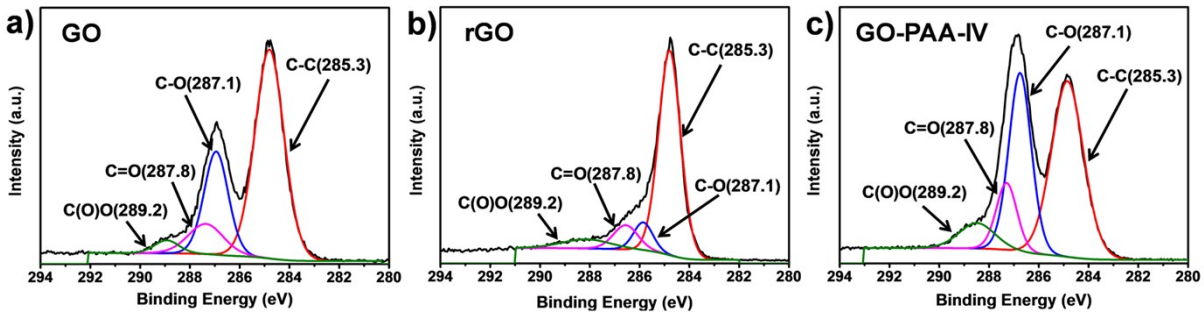

Figure S7. XPS spectra of pure GO (a) and rGO (b) film and GO-PAA-IV (c) composite. The C_{1s} broad peek could be fitted into four peaks at 285.3eV, 287.1eV, 287.8eV and 289.2eV corresponding to C-C, C-O, C=O and C(O)O groups, respectively.

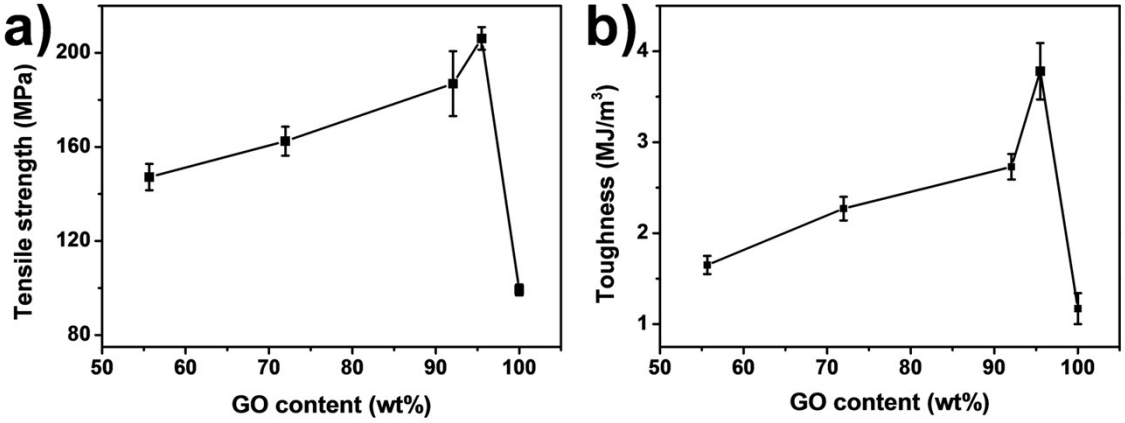

Figure S8. Tensile strength and toughness of GO-PAA nanocomposites with different GO contents.

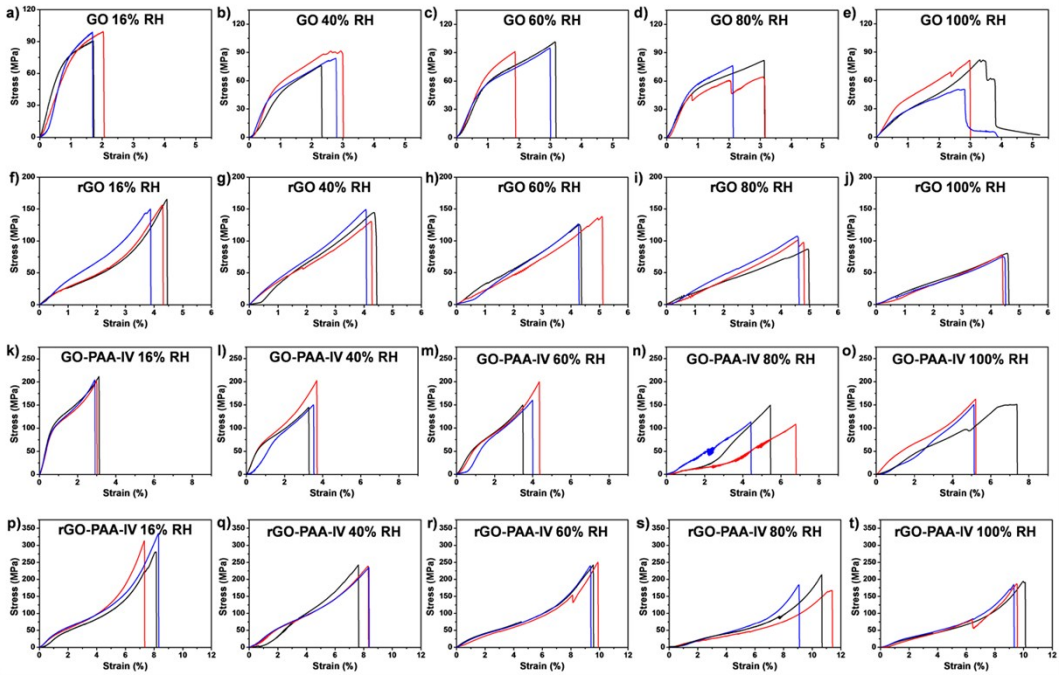

Figure S9. Typical tensile stress-strain curves of pure GO and rGO films, GO-PAA-IV and rGO-PAA-IV nanocomposites under different environmental relative humidity: a)~e) pure GO films under relative humidity of 16%, 40%, 60%, 80%, 100%; f)~j) pure rGO films under relative humidity of 16%, 40%, 60%, 80%, 100%; k)~o) GO-PAA-IV nanocomposites under relative humidity of 16%, 40%, 60%, 80%,100%; and p)~t) rGO-PAA-IV nanocomposites under relative humidity of 16%, 40%, 60%, 80%,100%.

Table S1. The weight loss of pure GO film, pure PAA film and GO-PAA nanocomposites between 100°C and 600°C; The exact GO content of GO-PAA nanocomposites were determined by TGA under nitrogen with a temperature rising rate of 10 $K \cdot min^{-1}$

Sample	Weight loss between 100°C and 600°C (wt%)	Input GO content (wt%)	GO content by TGA (wt%)
GO	41.72	-	-
GO-PAA-IV	43.13	95	95.49
GO-PAA-III	44.20	90	92.06
GO-PAA-II	50.48	70	71.97
GO-PAA-I	55.58	50	55.65
PAA	72.97	-	-

Table S2. The *d-spacing* of the GO-PAA and rGO-PAAnanocomposites with different GO contents before and after HI reduction.

Sample	d(Å)	
	Before HI reduction	After HI reduction
GO	7.70	3.72
GO-PAA-IV	7.80	3.75
GO-PAA-III	7.88	3.80
GO-PAA-II	8.14	3.90
GO-PAA-I	8.82	3.92

Table S3. The O_{1s}/C_{1s} atomic ratios by XPS and I_D/I_G by Raman spectra of GO film and GO-PAA-IV nanocomposite before and after HI reduction.

Sample	XPS	Raman
	O_{1s}/C_{1s} (atomic ratios)	I_D/I_G
GO	0.33	0.86
GO-PAA-IV	0.47	1.29
rGO	0.15	2.28
rGO-PAA-IV	0.36	2.39

Table S4. The mechanical properties of GO-PAA and rGO-PAA nanocomposites with different GO contents.

Sample	Tensile strength (MPa)	Modulus (GPa)	Strain (%)	Toughness (MJ/m^3)
GO	99.18 ± 2.31	10.93 ± 2.09	1.86 ± 0.18	1.17 ± 0.17
rGO	157.27 ± 7.81	4.45 ± 0.42	4.21 ± 0.29	2.69 ± 0.06
GO-PAA-I	147.17 ± 5.61	10.44 ± 1.52	2.08 ± 0.12	1.65 ± 0.10
rGO-PAA-I	205.31 ± 3.98	4.96 ± 0.23	4.73 ± 0.40	4.39 ± 0.27
GO-PAA-II	162.43 ± 6.15	10.50 ± 0.87	2.29 ± 0.11	2.27 ± 0.13
rGO-PAA-II	233.06 ± 10.59	3.75 ± 1.54	6.79 ± 0.77	6.75 ± 0.56
GO-PAA-III	186.89 ± 13.78	14.90 ± 0.62	2.51 ± 0.07	2.73 ± 0.14
rGO-PAA-III	264.10 ± 20.86	3.42 ± 0.53	7.84 ± 0.35	7.18 ± 0.55
GO-PAA-IV	206.12 ± 4.79	18.19 ± 2.14	3.01 ± 0.12	3.78 ± 0.31
rGO-PAA-IV	309.57 ± 27.00	4.57 ± 0.21	7.92 ± 0.52	8.88 ± 1.13

Table S5. The mechanical properties of pure GO and rGO films, GO-PAA-IV and rGO-PAA-IV nanocomposites under different environmental relative humidity.

Sample	Environmental relative humidity (% RH)	Tensile strength (MPa)	Modulus (GPa)	Strain (%)	Toughness (MJ/m^3)
GO	16	99.18 ± 2.31	10.93 ± 2.09	1.86 ± 0.18	1.17 ± 0.17
	40	83.72 ± 7.70	7.37 ± 1.62	2.67 ± 0.33	1.47 ± 0.41
	60	95.93 ± 5.30	7.40 ± 0.25	2.66 ± 0.70	1.65 ± 0.52
	80	74.12 ± 8.96	6.27 ± 0.51	2.77 ± 0.57	1.42 ± 0.33
	100	71.31 ± 17.79	4.19 ± 0.74	3.02 ± 0.26	1.41 ± 0.39
rGO	16	157.27 ± 7.81	4.45 ± 0.42	4.21 ± 0.29	2.69 ± 0.06
	40	141.48 ± 9.62	4.39 ± 0.66	4.22 ± 0.15	3.00 ± 0.19
	60	130.07 ± 6.89	3.22 ± 0.60	4.55 ± 0.47	2.82 ± 0.40
	80	98.55 ± 10.35	2.56 ± 0.45	4.70 ± 0.21	2.29 ± 0.12
	100	78.01 ± 2.54	2.13 ± 0.06	4.47 ± 0.09	1.70 ± 0.15
GO-PAA-IV	16	206.12 ± 4.79	18.19 ± 2.14	3.01 ± 0.12	3.78 ± 0.31
	40	165.81 ± 31.70	8.80 ± 0.86	3.49 ± 0.21	3.13 ± 0.66
	60	169.86 ± 26.21	7.30 ± 0.16	3.93 ± 0.44	3.38 ± 0.71
	80	126.95 ± 28.35	3.43 ± 0.62	5.55 ± 1.18	2.63 ± 0.29
	100	155.04 ± 6.47	3.22 ± 0.51	5.90 ± 1.28	4.39 ± 1.30
rGO-PAA-IV	16	309.57 ± 27.00	4.57 ± 0.21	7.92 ± 0.52	8.88 ± 1.13
	40	239.05 ± 3.63	3.40 ± 0.69	8.08 ± 0.44	8.32 ± 0.72
	60	244.40 ± 5.54	2.40 ± 0.46	9.60 ± 0.26	8.66 ± 0.19
	80	188.12 ± 23.15	1.71 ± 0.20	10.37 ± 1.17	6.48 ± 0.97
	100	179.03 ± 4.55	1.23 ± 0.30	9.60 ± 0.34	6.04 ± 0.49

Table S6. The mechanical properties of the natural nacre and other GO-based nanocomposites.

Layered Materials	Tensile strength (MPa)	Toughness (MJ/m^3)	Reference
Nacre	200.0	2.6	[13]
GO-PMMA	148.3	2.35	[6]
rGO-PVA	188.9	2.52	[7]
rGO-SL	300.0	2.80	[24]
GO-Ca^{2+}	125.8	0.31	[8]
GO-Mg^{2+}	80.6	0.13	[8]
GO-GA	101.0	0.30	[10]
GO-Borate	185.0	0.14	[9]
GO-PEI	209.9	0.23	[12]
rGO-PCDO	129.6	3.91	[21]
rGO-PDA	204.9	4.00	[20]
rGO-PAPB	382.0	7.50	[25]
rGO-MoS_2-TPU	235.0	6.90	[28]
rGO-PAA-IV	309.6	8.88	Our work